

## EXPERIMENTAL AND COMPUTATIONAL STUDIES OF STALL ON A HELICOPTER ROTOR AIRFOIL

**Katarzyna Surmacz**

*Institute of Aviation  
Department of Aerodynamics  
Krakowska Avenue 110/114, 02-256 Warsaw, Poland  
tel.: +48 228460011 ext. 360, fax: +48 228464432  
e-mail: katarzyna.surmacz@ilot.edu.pl*

### **Abstract**

*In the case of forward flight of a helicopter, the flow field around rotating blades of a rotor is highly three-dimensional and very complex. Helicopter blades work across a wide range of angles of attack and airspeed. The stall occurs on the retreating blade in forward flight and causes dissymmetry of lift on a rotor disc.*

*The investigation of the stall phenomenon has been performed using experimental and computational methods. Experimental analysis was made at the Ohio State University 6'x 22' unsteady transonic wind tunnel. Research in the wind tunnel was performed using two methods: oil visualization (over a wide range of  $\alpha$  and  $Ma$ ) and pressure measurements. Computational part of the research has been done using Computational Fluid Dynamics tool. 2- and 3-dimensional calculations performed using ANSYS FLUENT software. In both experimental and computational cases, the 3D flow around a section of a rotor blade based on the SSC-A09 airfoil was analysed. The test article of the research was a section, which was located in the tip region of the main rotor blade of UH-60M Black Hawk helicopter. The research was conducted for a wide range of angles of attack and at several velocities. The most interesting part of the analysis concerned on unsteady flow conditions corresponding to stall.*

**Keywords:** 3D flow, CFD, wind tunnel test, oil visualization, stall phenomenon

### **1. Introduction**

The advantage of helicopters over other aircraft is the ability to perform flights in each direction (forward, rearward, sideward, vertical). The nature of the airflow through the rotor depends of a state of flight. In hovering flight (Fig. 1a), a uniform constant distribution of thrust over the rotor disc is observed. The induced velocity along the blade span is azimuthally symmetric. In forward flight (Fig. 1b), the resultant velocity is the sum of the free stream  $V_\infty$  and the rotational velocity. The angle of attack ( $\alpha$ ) distribution is shown in Fig. 2. In this case, the flow field around rotating blades of a rotor is highly three-dimensional and very complex. Helicopter blades work across a wide range of angles of attack and airspeeds.

During high-speed flights on the retreating blade, the critical angle of attack can be exceeded causing the stall phenomenon [2, 4, 5, 7]. Its consequences are vibrations, pitch up of the nose and a rolling tendency. The retreating blade dynamic stall limits the maximum airspeed of a helicopter.

### **2. Methodology of investigation**

The nature of the flow field around a section of a rotor blade based on the Sikorsky SSC-A09 airfoil was investigated. The test article of the research was a section located in the tip region of the main rotor blade of UH-60M Black Hawk helicopter. The study was performed using experimental and computational methods. Experimental analysis was made in the Ohio State University 6'x 22' unsteady transonic wind tunnel (Fig. 3).

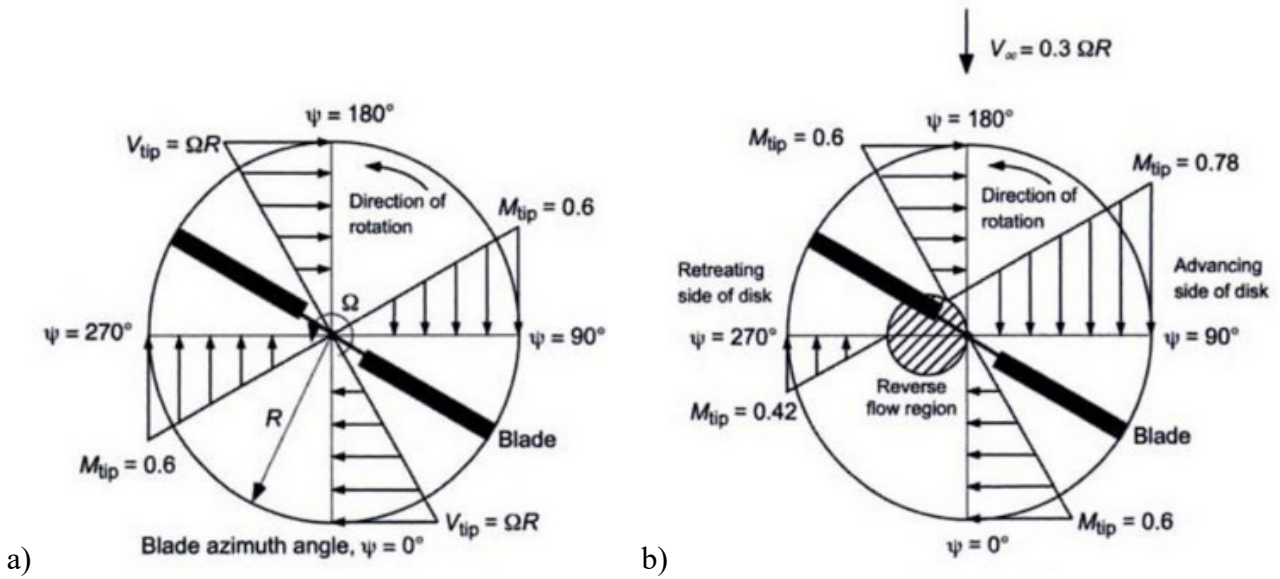


Fig. 1. Velocity distribution per rotor revolution [5]

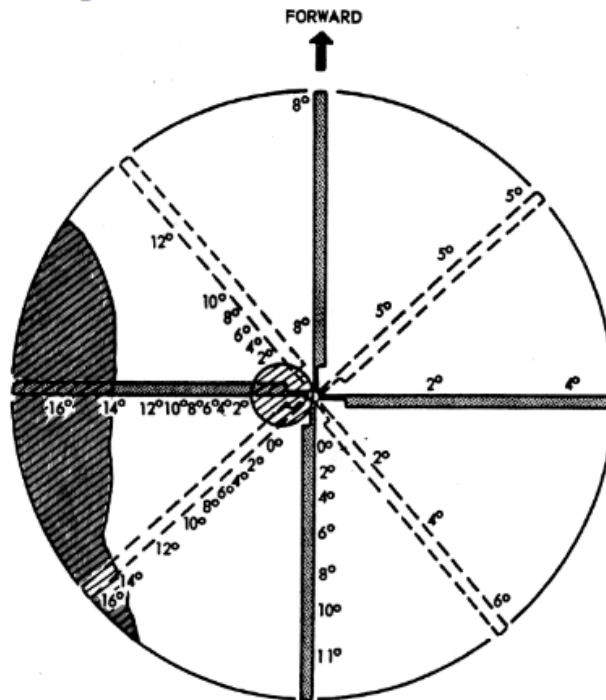


Fig. 2. Angle of attack distribution per rotor revolution [6]

The test section of the tunnel had a rectangular shape with height 22 in (56 cm), width 6 in (15 cm) and length 44 in (112 cm). Reynolds number and Mach number can be independently varied over defined range (Fig. 4). The test section is equipped with perforated floor and ceiling walls (6% porosity) for reducing Mach wave reflections in transonic flow.

The study of the flow around a section of blade was performed at angles of attack between 0 and 20 degrees and free stream Mach number  $Ma=0.2, 0.4, 0.6$ . The scale of the test model is shown in Fig. 5.

Research in the wind tunnel was performed using two methods: oil visualization (over a wide range of  $\alpha$  and  $Ma$ ) and pressure measurements. Oil visualization has been done using chalk dust on oil, which was distributed on the top surface of the airfoil. Fig. 6 illustrates the wing section before run. Process of the test was recorded using the high-speed camera.

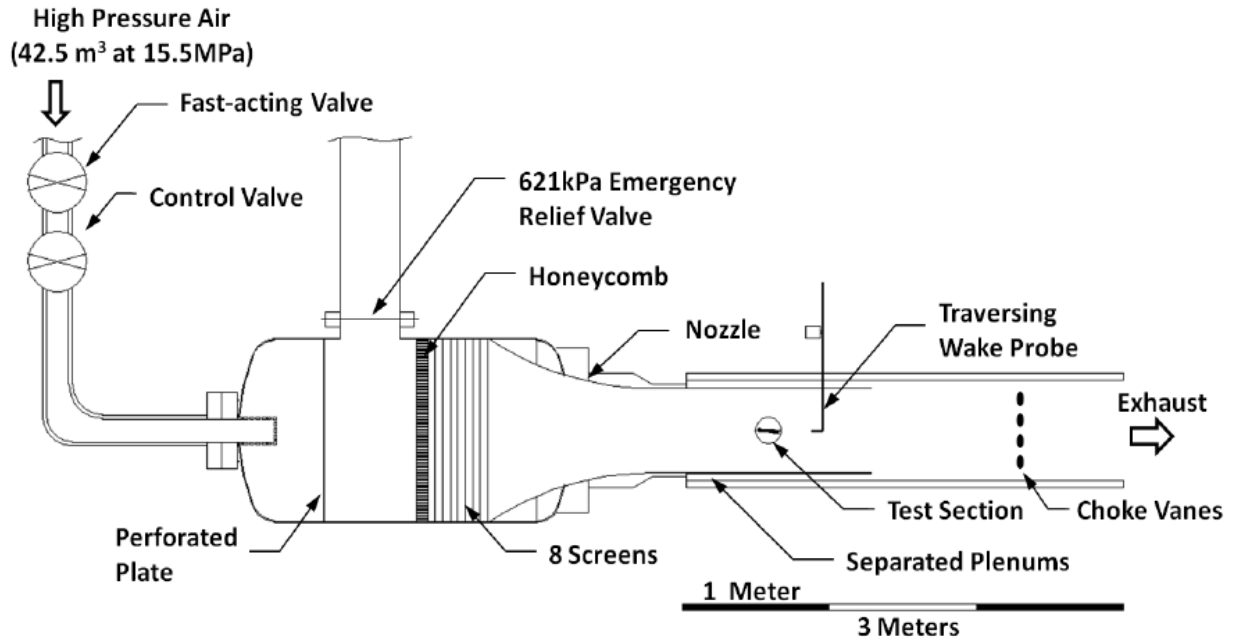


Fig. 3. Schematic of OSU 6'x 22'' wind tunnel [3]

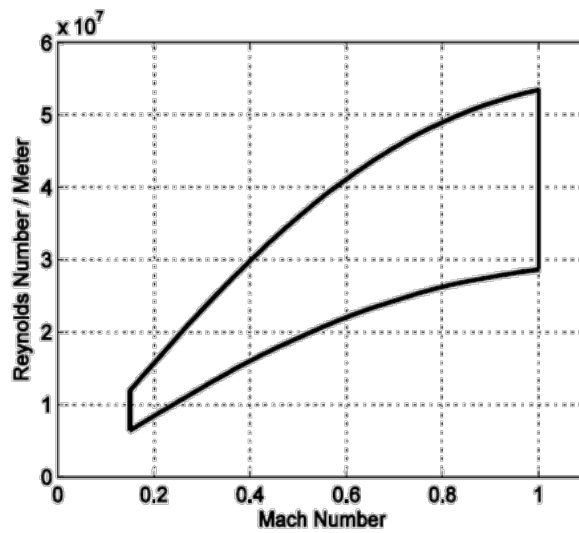


Fig. 4. Range of Re and Ma numbers OSU 6'x 22'' tunnel [3]

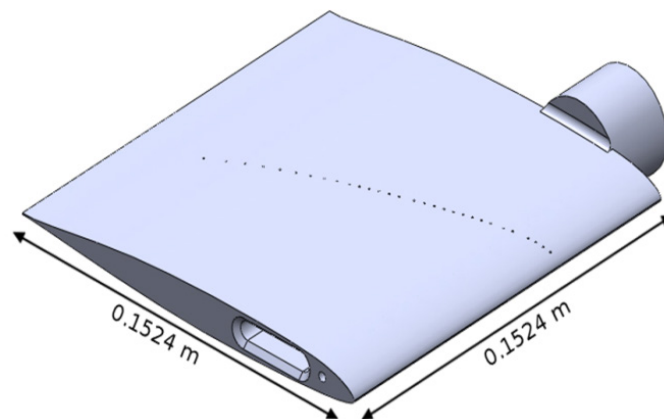


Fig. 5. Geometry of the test model

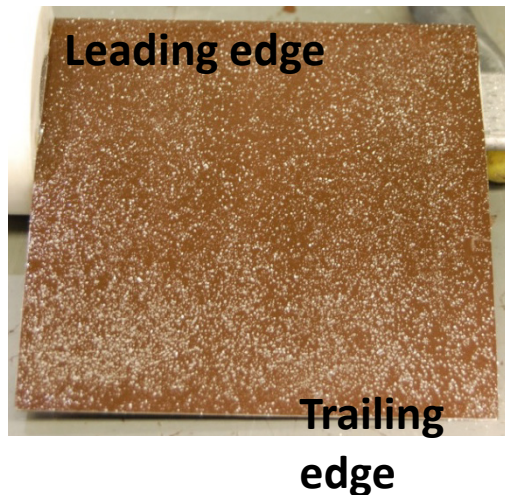


Fig. 6. The wing section before run

The computational part of the research has been done using Computational Fluid Dynamics tool. 2- and 3-dimensional calculations performed using ANSYS FLUENT software [1]. The fluid was simulated as a compressible with the Spalart-Allmaras turbulence model. Four computational models were prepared for analysis:

- 2 D farfield,
- 2D airfoil in wind tunnel with solid walls,
- 3D wing in wind tunnel with solid walls,
- 3D wing in wind tunnel with perforated walls.

2D simulations are the equivalent to an infinite wing. 3D models were created for investigate differences between an infinite wing and a wing with a low aspect ratio. Computational models allowed comparing the free-flight conditions with wind tunnel conditions. The computational mesh near the airfoil surface is presented in Fig. 7.

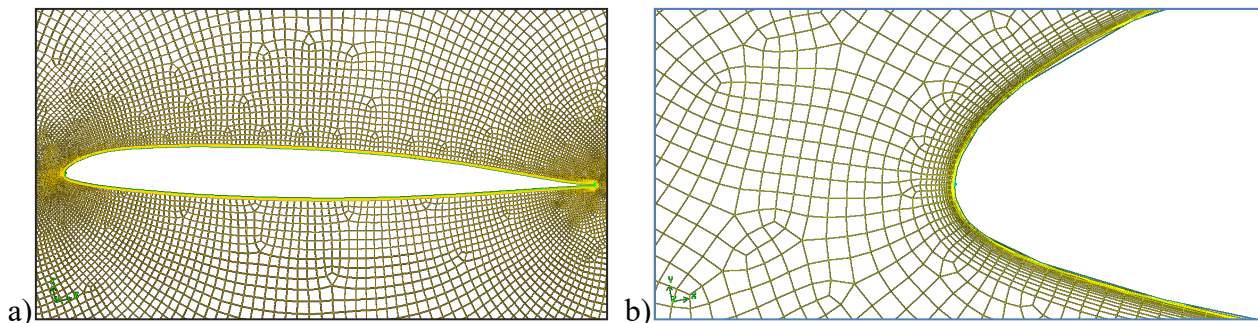


Fig. 7. Computational grid: a) around the airfoil; b) around a nose of the airfoil

### 3. Results

The aim of the work was the study of an initialization and growth of the stall process. For this investigation, two methods were applied: experimental (pressure measurements and oil visualization) and computational (CFD). The application of these techniques provided qualitative and quantitative information on the stall phenomenon.

In the first part of the investigation pressure measurement was performed. The results are presented in the paper [3]. Aerodynamic characteristics (lift coefficient, drag coefficient and moment coefficient versus angle of attack) at free stream Mach numbers  $Ma=0.2, 0.4, 0.6$  are shown in Fig. 8. As can be seen in graphs, for SSC-A09 airfoil the critical angle of attack is 15 degrees ( $Ma=0.2$ ) or less (for Mach number greater than 0.2).

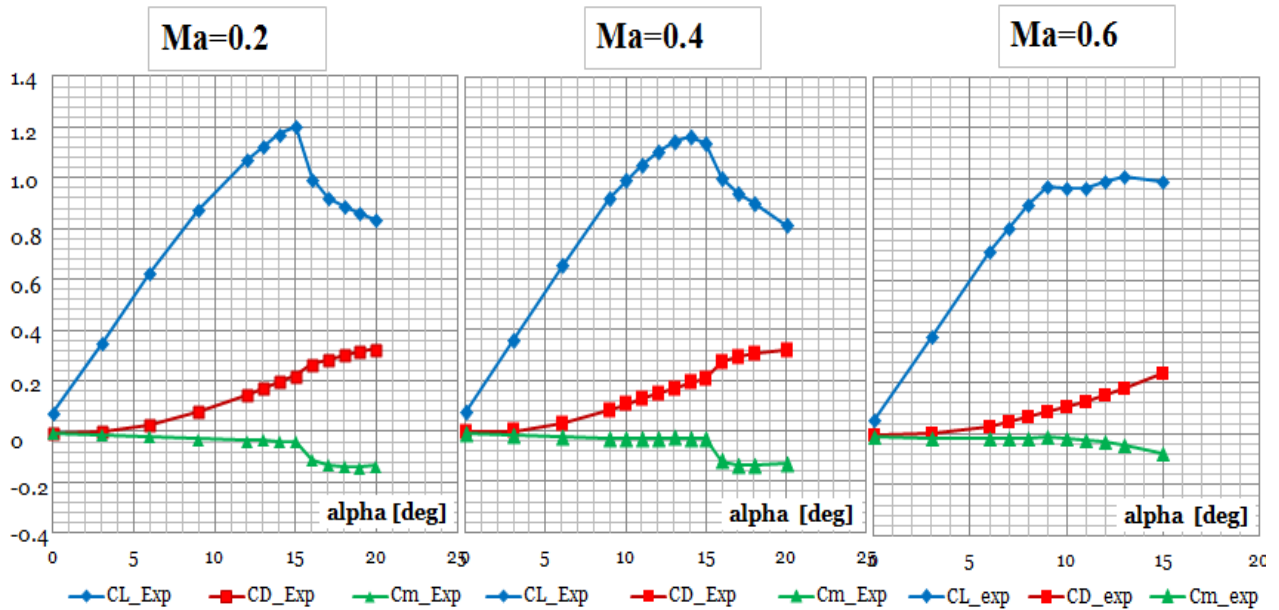


Fig. 8. Experimental aerodynamic characteristics of an SSC-A09 airfoil [3]

In the next part of the investigation, flow conditions corresponding to light stall, deep stall and post stall were simulated using wing tunnel tests and CFD. At low angles of attack attached, symmetric, steady flow is observed on the top surface of the airfoil. The flow behaviour near stall conditions is noted at  $Ma=0.2, \alpha=12^\circ$  (Fig. 9). The airflow in front of the airfoil was undisturbed and two-dimensional. Behind the separation line (about 75% of the chord at the middle span) three-dimensional, turbulent flow is observed. The reversed flow in the central part of the wing appeared.



Fig. 9. Oil flow visualization for  $Ma=0.2, \alpha=12^\circ$

Stall conditions were observed for the angle of attack close to 15 degrees. The computational and experimental results showed a similar pattern on the top surface of the airfoil (Fig. 10-11). The important features of the flow are the separation line near the leading edge, the reverse flow region in the middle part of the wing, vortices near the side edges of the wing as the effect of sidewalls of the wind tunnel.

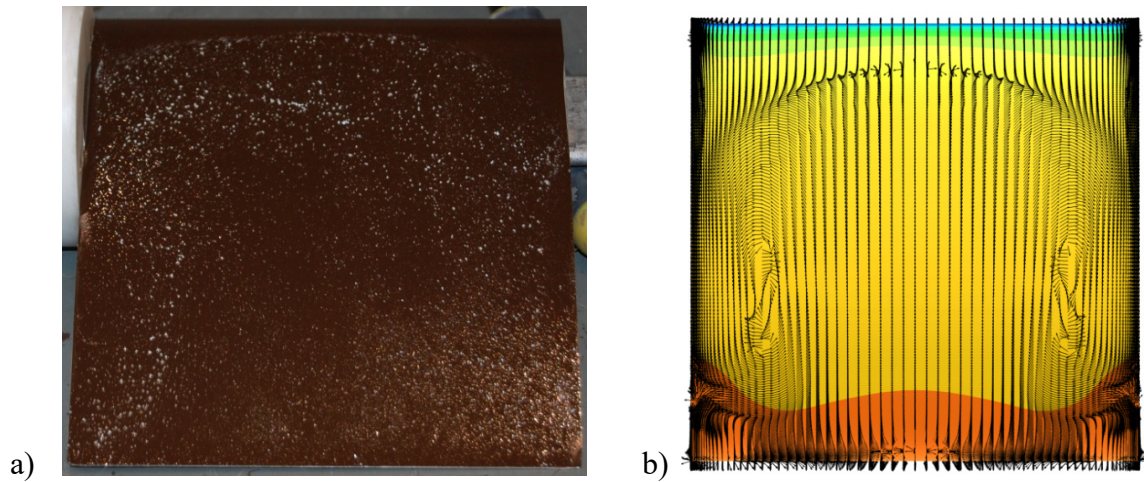


Fig. 10. Flow visualization: a) experimental –  $Ma=0.2$ ,  $\alpha=15^\circ$ ; b) computational –  $Ma=0.2$ ,  $\alpha=15^\circ$

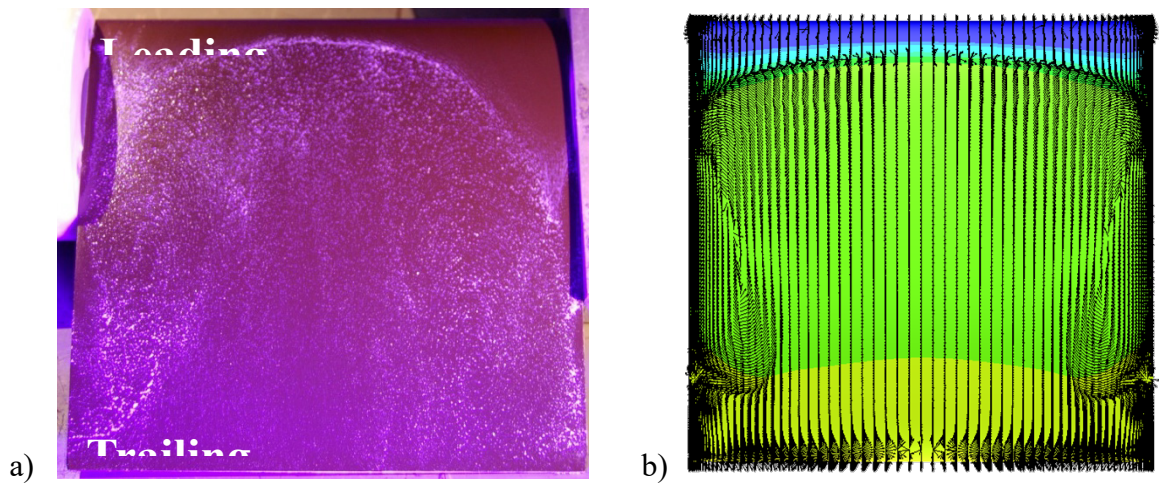


Fig. 11. Flow visualization: a) experimental –  $Ma=0.4$ ,  $\alpha=16^\circ$ ; b) computational –  $Ma=0.4$ ,  $\alpha=15^\circ$

At angles of attack higher than 14 degrees three-dimensional disturbed flow was observed. The separation line is closer to the leading edge than previously. As can be seen in Fig. 12, an asymmetric flow due to different sidewalls attachments was noted. For angle of attack higher than critical the strong three-dimensional flow effect occurred.

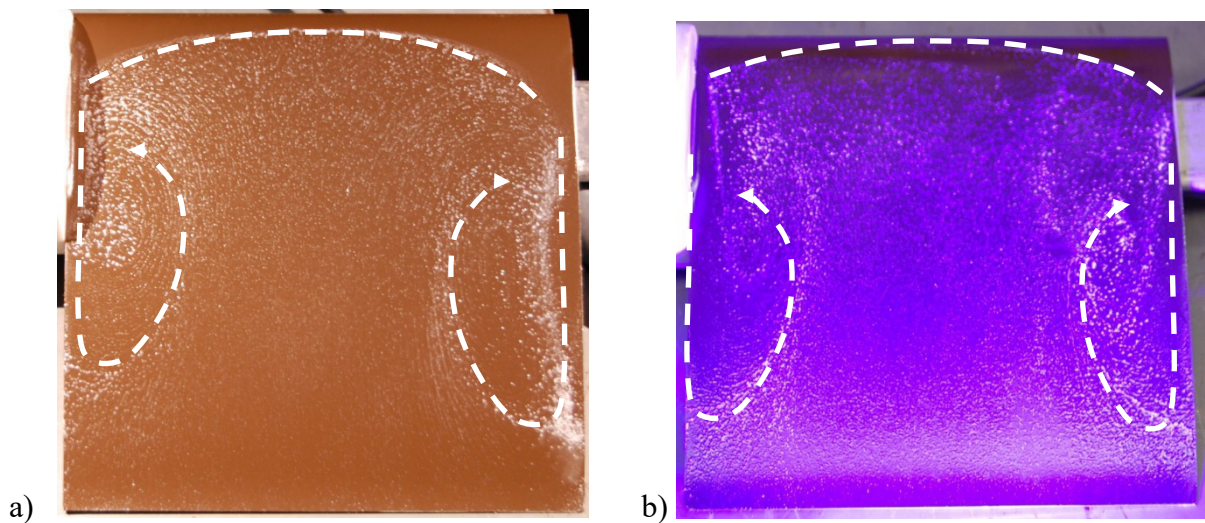


Fig. 12. Oil flow visualization: a)  $Ma=0.4$ ,  $\alpha=18^\circ$ ; b)  $Ma=0.4$ ,  $\alpha=20^\circ$

#### 4. Conclusions

The objective of the work was the investigation of the negative effect of stall on a helicopter rotor airfoil (Sikorsky SSC-A09). In order to understand the stall phenomenon, two research tools were used: experimental (wind tunnel testing) and computational (CFD). Both methods showed the stall region for the same range of angles of attack. The results of computational studies showed that 3D CFD model with perforated walls is more appropriate to simulate the flow in the test section of the 6x22 wind tunnel. Computational models have sufficient accuracy to simulate dynamic stall with Mach or pitch oscillation.

#### References

- [1] ANSYS FLUENT, *Theory guide*, 2012.
- [2] Bazov, D. I., *Helicopter aerodynamics*, Transport Press, Moskwa 1969.
- [3] Hird, K., Frankhouser, M. W., Gregory, J., Bons, J. P., *Compressible dynamic stall of an SSC-A09 airfoil subjected to coupled pitch and freestream Mach oscillations*, AHS 70<sup>th</sup> Annual Forum, 2014.
- [4] Krzyżanowski, A., *Mechanika lotu śmigłowca*, Wojskowa Akademia Techniczna, Warszawa 2010.
- [5] Leishman, G. J., *Principles of helicopter aerodynamics*, Cambridge University Press, 2002.
- [6] Marques, F. D., *Principles of rotorcraft flight*, 2012.
- [7] Seddon, J., *Basic helicopter aerodynamics*, BSP Professional Books, Oxford 1990.

